# Current fluctuations in rough superconducting tunnel junctions

Georg Heinrich[1,2] and F. K. Wilhelm[2,*]

[1]*Physics Department, Arnold Sommerfeld Center for Theoretical Physics and Center for NanoScience, Ludwig-Maximilians-Universität, Theresienstrasse 37, 80333 Munich, Germany*

[2]*IQC and Department of Physics and Astronomy, University of Waterloo, 200 University Avenue West, Waterloo, Ontario, Canada N2L 3G1*

Intrinsic noise is known to be ubiquitous in Josephson junctions. We introduce a rough tunnel junction model characterized by a very small number of pinholes—transport channels possessing a transmission coefficient close to unity and analyze its transport properties. Although it may still have just a small total leakage current, it can lead to enormous current fluctuations in the low-voltage regime. We show that even fully transparent transport channels between superconductors contribute to shot noise due to the uncertainty in the number of Andreev cycles. We discuss shot-noise enhancement by multiple Andreev reflection in such a junction and investigate whether pinholes might contribute as a microscopic mechanism of two-level current fluctuators. We discuss the connection of these results to the junction resonators observed in Josephson phase qubits.

## I. INTRODUCTION

Implementing qubits using superconducting circuits[1,2] is one of the most promising approaches to design a quantum computer. Various implementation schemes have been developed.[3–10] The crucial and indispensable device in all these setups is a Josephson tunnel junction. Hence, microscopic understanding of this kind of junction and all possible details is essential to advance this field. Current fluctuations in Josephson Junctions, as they are discussed in this paper, are of particular importance as they contribute to decoherence.

### A. Decoherence, 1/f noise

One of the major challenges for the realization of practical quantum computing is to perform a sufficient number of quantum manipulations within the coherence time. The need to maintain quantum coherence during the operation is especially difficult to achieve in solid-state systems which couple relatively strongly to uncontrollable environmental degrees of freedom that generate quick decoherence.

After electromagnetic qubit environments have been successfully engineered to improve coherence, we are now mostly concerned with intrinsic noise of the solid-state system. The most prominent source of intrinsic decoherence is non-Gaussian $1/f$ noise,[11] for which the spectral function behaves like $S(\omega) \propto 1/\omega$.[12,13] $1/f$ noise typically appears due to slowly moving defects in strongly disordered materials and is usually explained by an ensemble of two-level fluctuators coupling to the system under consideration. A heat bath causes uncorrelated switching events between the two states, which are described by a Poissonian distribution with mean switching time $\tau$. For a single fluctuator this leads to *random telegraph noise* (RTN). Superimposing several such fluctuators, using an appropriate mean switching time distribution $\rho(\tau)$, results in a $1/f$ noise spectrum. $1/f$ noise seriously limits the operation of superconducting qubits.[14–16]

Besides magnetic-flux fluctuations,[17,18] critical-current fluctuations due to charge trapping at defects in the tunnel barrier[14] or glassy fluctuations[19] are prominent, possible mechanisms for low-frequency $1/f$ noise in junctions of superconducting qubits. As complement to this, we will investigate the intrinsic noise of Josephson tunnel junctions containing a few high-transmission channels that potentially reside in the junction. We will address the question whether such defects might introduce another intrinsic source of current fluctuations leading to $1/f$ noise.

### B. Rough superconducting tunnel junctions

A Josephson tunnel junction consists of two superconductors separated by a thin insulating oxide layer. Transport through such a contact can be described by quantum-transport channels[20] which, in our case, refer to the channels of the oxide.

In tunnel junctions, the transmission $T$ of all transport channels are assumed to be small. However, the fabrication process is usually not at all epitaxial quasiequilibrium growth, thus one has to expect the oxide layer to be noncrystalline and disordered.[21,22] We will take this into account by investigating *rough superconducting tunnel junctions*, where we assume that the junction additionally contains a few transport channels with very high-transmission eigenvalues. *Pinholes*, see Fig. 1, might occur as defects due to the fabrication process. Indeed, in Ref. 23, the importance of pinholes was pointed out but also Ref. 24 discusses the significance of pinholes in mesoscopic devices, e.g., for the Kondo effect.

There has been previous interest in pinholes to understand subharmonic gap structure in weak links. In Ref. 25 the subharmonic gap structure of a tunnel junction was modeled by assuming that some channels have pinhole character. Analyzing superconducting qubits containing pinholes has additional motivations that are going to be reviewed in the following sections.
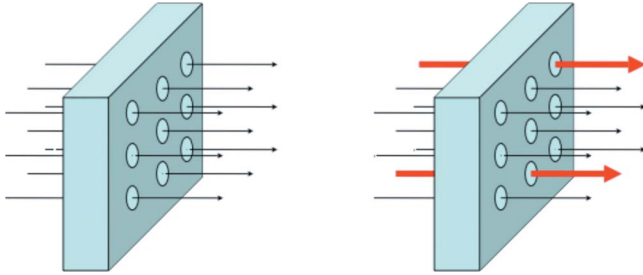
FIG. 1. (Color online) Schematic of the oxide layer of a Josephson Junction. Several transport channels are indicated. The arrow thickness corresponds to the respective transmission eigenvalue. Left: schematic of an ideal Josephson tunnel junction. The transmission of all channels is small. Right: considered *rough Josephson tunnel junction*, i.e., a tunnel junction including some high-transmission channels, so-called pinholes.

### 1. Multiple Andreev reflections (MAR)

In Josephson junctions with voltage bias $V$ smaller than the superconducting gap $2\Delta$, direct tunneling of quasiparticles is impossible. In this case, charge transport is governed by MAR.

Conventional Andreev reflection[26,27] is usually depicted at the interface between a normal and a superconductor: For voltage bias smaller than the superconducting gap, electrons have insufficient energy to be transferred as quasiparticles. Charge from the normal conductor can only be transmitted in a higher-order process where an electron, simultaneously with a second one of adequate energy and momentum, generates an additional Cooper pair. Hence, in this process, *two* electrons are transferred simultaneously and the second, now absent electron in the normal conductor, appears as a reflected hole.

In a Josephson junction, there are two superconductor-scatterer interfaces where Andreev reflection can take place. This might lead to processes involving a sequence of Andreev reflections or a cycle between the two interfaces, i.e., MAR.[27–29] Schematically, one might imagine the reflected hole due to Andreev reflection at one interface, to be reflected again in a subsequent step at the other interface and so on. Because of the voltage bias $V$ each step of this cycle corresponds to an energy gain $eV$. Thus, for a sufficient large number of reflections, the energy gap $2\Delta$ can be overcome and the process transfers multiple-charge quanta at a time. In general, an $n$th order MAR process comprises $(n-1)$ reflections and transfers $n$ charge quanta simultaneously, a so-called *Andreev cluster*. The $n$ steps of the cycle correspond to a total-energy gain $neV$. Thus, for voltage bias $V$, only processes with $n \geq 2\Delta/eV$ can gain enough energy to overcome the energy gap. Consequently, the $n$th order MAR process only occurs above the threshold voltage $V_n = 2\Delta/(en)$ and for given bias $V$, charge is only transferred in quanta of size bigger or equal $(\lfloor 2\Delta/eV \rfloor + 1)$, where $\lfloor x \rfloor \equiv \max_{k \leq x, k \in \mathbb{Z}}(k)$.

Because these MAR processes are composed of multiple transmission cycles, they sensitively depend on the electron-transmission probability, i.e., the set of transmission eigenvalues characterizing the junction. We thus expect that rough superconducting tunnel junctions will be highly affected by

MAR and we will see that even very few pinholes will have an extreme impact on the transport properties of the junction.

### 2. Noise enhancement due to MAR

In Ref. 23, shot noise[30] of NbN/MgO/NbN superconductor-insulator-superconductor tunnel junctions was measured. The result shows enhanced noise which is attributed to the occurrence of MAR processes in pinholes of the MgO barrier. They model their data assuming Poissonian shot noise $2eI$, where they replaced the single-charge quantum $e$ by an effective transferred charge $q(V)$ due to MAR.

Such processes might be highly relevant as a source of intrinsic noise in superconducting qubit devices due to pinholes residing in the Josephson junction. It has to be realized that in the case of transport through very high transmission channels, in general, shot noise is not governed by the simple Poisson formula $2eI$, which is only valid in the limit of small transmission. The method, we will use, properly treats all possible transmission eigenvalues.

### 3. Junction resonators

A new measurement revealing major intrinsic sources of decoherence in Josephson-junction qubits was performed in Ref. 31. The authors observed characteristics of energy-level repulsion at certain frequencies as predicted for coupled two-state systems. This structure of level splittings was attributed to spurious resonators residing in the Josephson junction. Measurements of Rabi oscillations revealed that these resonators cause significant decoherence.[32] Similar to the scenario of charge trapping, mentioned before with respect to $1/f$ noise, the energy-level repulsion could be explained by assuming two-state current fluctuators in the junction.

Although other processes, such as charge trapping within the junction barrier, are believed to be relevant effects for realizing such spurious resonators, pinholes in rough tunnel junctions might be additional candidates for introducing two-state current fluctuators, see Sec. V B.

The structure of this paper is as follows: after a short survey of the method used, we discuss leakage current of rough superconducting tunnel junctions. This is followed by a section regarding its noise properties. Finally we investigate the full counting statistics of pinholes to discuss whether they might contribute as a microscopic mechanism of two-level current fluctuators.

## II. METHOD

To investigate rough superconducting tunnel junctions we have to use an approach that equally well considers small-*and* high-transmission channels of the oxide separating the two voltage-biased superconductors. Perturbative approaches are insufficient. Second, in order to discuss pinholes as possible junction resonators, we need sufficient insight into the transport process to examine such non-Gaussian noise sources. The calculation of the *full counting statistics* (FCS) in terms of the nonequilibrium Keldysh Green's function approach[33] achieves both.

The FCS of charge transfer is the probability distribution $\mathcal{P}_{t_0}(N)$ for a total number of $N$ charge quanta to be transmitted within measurement time $t_0$.[34–36] Just as well, we can consider the *cumulant generating function* (CGF) $\mathcal{C}_{t_0}(\chi)$ with $\exp[\mathcal{C}_{t_0}(\chi)] = \Sigma_N \mathcal{P}_{t_0}(N)\exp(iN\chi)$. Here, $\chi$ is an auxiliary variable, the *counting field*. The use of Keldysh Green's functions is particularly useful in the case of nonequilibrium superconductors and allows to employ several quantum field-theoretical methods from transport theory of metals.[37] This way the effect of small and high-transmission channels can be accurately taken into account as needed. Additionally $\mathcal{P}_{t_0}$ itself includes information beyond Gaussian noise distributions as it allows to calculate higher, non-Gaussian cumulants, $c_n = (-i)^n [\partial^n \mathcal{C}_{t_0}/\partial \chi^n]_{\chi=0}$, such as they occur in RTN. This is necessary to discuss junction resonators.

For a single-mode Josephson Junction biased by a voltage $V$ the CGF was calculated analytically in Refs. 38 and 39. We extend this result to multimode junctions containing multiple transport channels which are characterized by a set of arbitrary transmission eigenvalues $\{T_m\}$, in particular, to our rough junction model. We restrict ourselves to the zero-temperature case. Given the work done in Refs. 38 and 39 we immediately find for the CGF in our case

$$\mathcal{C}_{t_0}(\chi) = \frac{2t_0}{h}\sum_m \int_0^{eV} dE \times \ln\left[1 + \sum_{n=0}^{\infty} P_n(E,V,T_m)(e^{in\chi}-1)\right].$$
(1)

$P_n(E,V,T_m)$ is the probability for an $n$th order MAR-process transferring $n$ charge quanta simultaneously through a channel of transmission $T_m$ with voltage bias $V$ at energy $E$. The basic steps of the calculation leading to Eq. (1) are summarized in Appendix.

## III. LEAKAGE CURRENT

We quantitatively investigate *leakage current*, i.e., current in the subgap voltage regime $eV < 2\Delta$ of a rough superconducting tunnel junction. Using Eq. (1) and $\langle N \rangle = -i[\partial \mathcal{C}_{t_0}/\partial \chi]_{\chi=0}$, the average current $I$ of our junction, containing $M$ transport channels characterized by a set of transmission eigenvalues $\{T_m\}$ which is described by the distribution $\rho(T)$, is given by

$$I = \frac{2e}{h}M\int_0^1 dT\rho(T)\int_0^{eV} dE \sum_n nP_n(E,V,T).$$
(2)

### A. Homogeneous multimode contacts

For illustrative reasons we start from a homogeneous multimode contact between superconductors containing $M$ transport channels all with the same transmission eigenvalue $T_1$. The transmission eigenvalue distribution reads $\rho(T) = \delta(T - T_1)$. In the case $M=1$, this would be a single-mode quantum point contact (QPC). We compute conductance in units of the normal-state conductance $G_N = \frac{2e^2}{h}M\int dT\rho(T)$. From Eq. (2) it is clear that the normalized average current of a homogeneous multimode contact is, besides the obvious
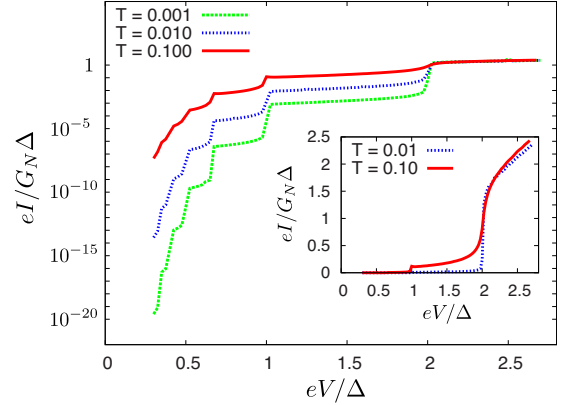


FIG. 2. (Color online) Current through a homogeneous multimode contact with small transmission between superconductors as a function of bias voltage, at zero temperature, on a logarithmic current scale. Inset: linear current scale.

scaling with the channel number $M$, the same as the one of a single-mode QPC which was already discussed in Ref. 39.

For small-transmission eigenvalues, Fig. 2 shows the average current as a function of bias voltage for low-transmission probability $T_1 \ll 1$ on a logarithmic and linear scale. We see that a contact with $T_1 = 0.1$ already develops a relatively large leakage current in the subgap regime $eV < 2\Delta$. Another immediate aspect, which will become important below, is its scaling. Conductance steps of size $T_1$ arise at MAR voltages $2\Delta/n$, demonstrating that the current is reduced by a factor of $T_1$ at each step. For a single-mode QPC it was shown before that current transport for small-transmission eigenvalues in the voltage interval $[2\Delta/(ne), 2\Delta/(n-1)e]$ is dominated by the $n$th-order MAR process. In Ref. 39 the authors explicitly showed this $T^n$ dependence within a perturbative calculation.

For high-transmission contacts we note that perturbative approaches in $T$ will fail and it is necessary to use nonperturbative methods as mentioned above. This is, in particular, important for deriving quantitative results for rough junctions containing low- and high-transmission channels. Figure 3 shows the current for a range of transmission probabilities $T \geq 0.6$. Especially at small voltages, the current through high-transmission modes is larger by orders of magnitude compared to the small-transmission case.

### B. Rough tunnel junctions

We now turn to rough Josephson tunnel junctions assuming a small number of pinholes with transmission eigenvalues close to unity that reside in the junction. We consider a contact with $M$ channels. A fraction $a$ of these channels has a high-transmission eigenvalue $T_1$, the vast majority has a small value $T_2$, typical for tunnel contacts. Altogether, we consider the eigenvalue distribution

$$\rho(T) = a\,\delta(T - T_1) + (1-a)\,\delta(T - T_2)$$
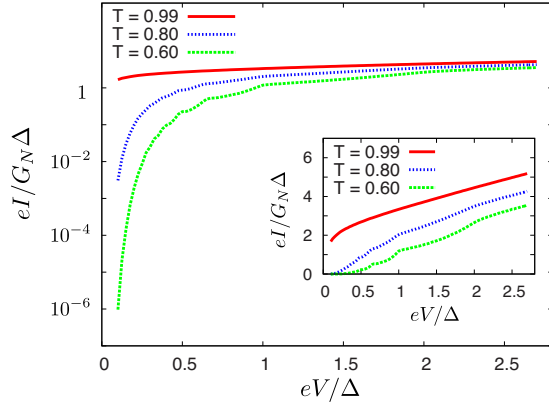(3)

causing a normal conductance of

FIG. 3. (Color online) Current through a homogeneous multi-mode contact with high transmission between superconductors as a function of bias voltage, at zero temperature, on a logarithmic current scale. Inset: linear current scale.

$$G_N = \frac{h}{2e^2} M[aT_1 + (1-a)T_2].$$

In Sec. III C we are going to discuss why this distribution captures the essential physics of more complicated distributions.

We calculate the current for this model, taking into account the very different transport properties of $T_1$ and $T_2$ channels. The result for two scenarios with extremely small pinhole fraction $a$ is shown in Fig. 4. We see that, starting at high voltages, the current follows the well-known subharmonic gap structure curve for tunnel-transmission coefficient $T_2$ only above a certain voltage, depending on $a$. However, below that voltage, due to the fact that the current carried by tunnel-transmission channels is reduced by a factor of $T_2$ each time the voltage passes another MAR voltage $V_n = 2\Delta/n$, the highly transmissive channels dominate, leading to a smooth, weakly structured subgap contribution that level off into a plateau before it drops again. Consequently, at
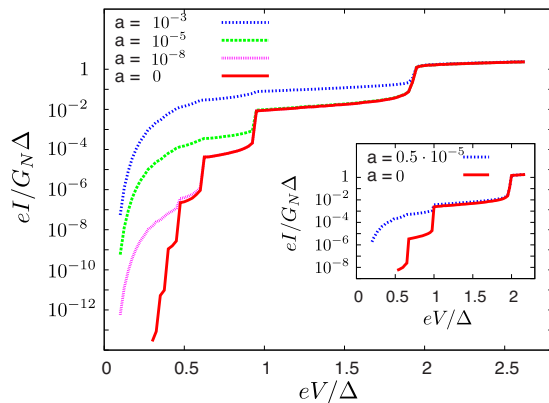


FIG. 4. (Color online) Leakage current on a logarithmic scale as a function of bias voltage, at zero temperature, for a rough superconducting tunnel junction with transmission eigenvalue distribution $\rho(T) = a\delta(T-T_1) + (1-a)\delta(T-T_2)$, $T_1 = 0.6$, and $T_2 = 0.01$. Inset: $T_1 = 0.6$ and $T_2 = 0.003$. The different curves refer to different pinhole fractions $a$ within all transport channels.

sufficiently low voltages, the leakage current through rough tunnel contacts is mostly carried by the pinhole fraction. Nevertheless, in general, it is still very small compared to the current at voltages above the gap.

Our quantitative treatment provides insight into the pinhole fraction $a$ which[25] seems to overestimate. Indeed, from Fig. 4, for example, we infer that in a junction, where two full current steps at $eV = 2\Delta$ and $eV = 2\Delta/2$, each scaling with a factor of 0.01, are observed, we only have a pinhole fraction of less than 1 out of $10^6$ channels with pinhole transmission $T \gtrsim 0.6$.

### C. Characterizing pinhole thresholds

As we have seen, below a certain voltage, a high-transmission channel residing in a rough Josephson tunnel junction dominates high-order subharmonic steps in the current characteristic. We can use this result to characterize the fraction of pinholes in all transmission channels by very sensitive current measurements.

In Ref. 40 a current-voltage plot for an Al-Al$_2$O$_3$-Al junction used in a Josephson-junction qubit is presented. At $eV = 2\Delta$ the measured current shows a subharmonic step corresponding to a tunnel transmission eigenvalue of $T = 0.003$. The second current drop at $eV = \Delta$ is indicated but the measurement does not resolve the next expected plateau. The experimental result is consistent with the calculation presented in the inset of Fig. 4 for a pinhole fraction $a = 0.5 \times 10^{-5}$. This corresponds to one pinhole of $T_1 = 0.6$ in a junction of $1/a = 200\,000$ channels. Actually, in Ref. 31, the number of transport channels for the junction under consideration[40] is estimated to this order of magnitude, indicating that the existence of pinholes in state-of-the-art superconducting qubit devices is compatible with current measurements.

Indeed, new design concepts have lead to a significant reduction in the junction size (see Ref. 41) and with it a suppression of intrinsic noise. Clearer insight would be provided by highly sensitive current-voltage measurements at voltages stretching out over several current steps at $V_n = 2\Delta/n$. In the following, we will assume a small number of pinholes.

Finally, this provides the justification for the very simple transmission distribution function, Eq. (3). The transmission eigenvalues are determined by WKB, $T = \exp(-\kappa d)$, and this way, depend on the junction thickness $d$. Then the pinhole-transmission eigenvalues might be related to a distribution of thickness $\rho(d)$ of the oxide layer separating the superconductors. Considering the strict non-negativity of $d$, a lognormal distribution might be appropriate for describing $\rho(d)$ for the pinholes. All this can be done in our approach but as we have seen above, in state-of-the-art superconducting qubit devices we might only have a small, single-digit number of pinholes in a huge junction. Thus, doing statistics is not necessary and considering a single value $T_1$ to represent the pinhole-transmission-eigenvalue distribution, as done in Eq. (3), is a sufficient way to take them into account.

### IV. NOISE

We will examine the noise properties of rough superconducting tunnel junctions. Current noise is defined in terms of
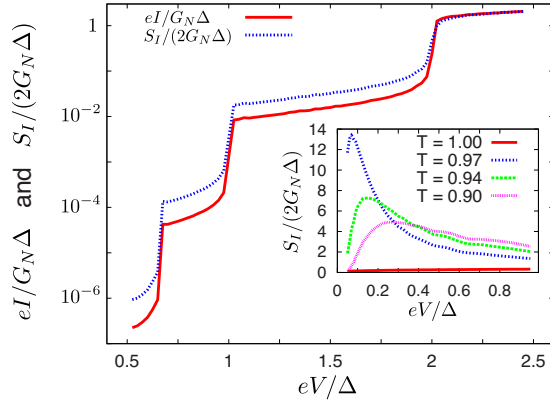
FIG. 5. (Color online) Noise and current as a function of bias voltage, at zero temperature, for a homogeneous superconducting tunnel junctions with transmission eigenvalue $T=0.01$. Inset: noise characteristics for junctions with large transmission.
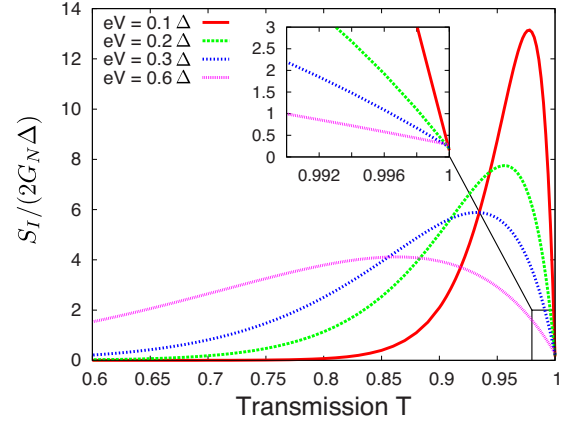


FIG. 6. (Color online) Noise $S_I$ as a function of transmission eigenvalue $T$ for a homogeneous superconducting tunnel junction where the bias voltage is set as parameter. Inset: enlargement around $T=1$.

the Fourier transform of the autocorrelation function of current fluctuations $\delta I(\tau)=I(\tau)-\langle I\rangle$. So the zero-frequency noise reads $S_I \equiv \int_{-\infty}^{\infty} d\tau \langle\{\delta I(\tau), \delta I(0)\}\rangle$. Transforming the second cumulant $c_2 = (N-\bar{N})^2 = \frac{1}{2e^2}\int_0^{t_0}\int_0^{t_0} dt dt' \langle\{\delta I(t), \delta I(t')\}\rangle$, where $N$ again refers to the total number of charge quanta transferred, to average $\bar{t}=(t+t')/2$ and relative $\tau=t-t'$ time coordinates, and assuming $t_0$ to be much longer than the current correlation times, the correlator above will not depend on $\bar{t}$. Executing both integrations we have $S_I = (2e^2/t_0)[\partial^2 \mathcal{C}_{t_0}/\partial\chi^2]_{\chi=0}$, and using the cumulant generating function (1), we finally find for the zero-frequency noise

$$S_I = \frac{4e^2}{h}\sum_m \int_0^{eV} dE \times \left\{ \sum_n n^2 P_n(E,V,T_m) - \left[\sum_n n P_n(E,V,T_m)\right]^2 \right\}. \quad (4)$$

### A. Homogenous multimode contacts

Again, as in Sec. III, we start from homogeneous multimode contacts, with each channel having the same transmission eigenvalue, and begin the discussion with small transmission $T \ll 1$. Figure 5 shows noise and current characteristics. In this case, there is always one very dominant MAR process, which causes charge transport to be dominated by quanta of $q(V)=e(1+\lfloor 2\Delta/eV\rfloor)$ and the noise scales with this additional charge factor. Thus, in the small-transmission regime Poissonian shot noise $S_I=2eI$ with modified charge quantum $nq(V)$, properly explains the observed noise features.

In the case of large-transmission eigenvalues, inset of Fig. 5, the noise characteristic changes dramatically. For very high probabilities $T$, the noise increases with decreasing voltage in the subgap regime. Depending on the value of $T$, it develops a maximum but falls off again at even lower $V$. Remarkably, and in strong contrast to any simpler model, we note that a contact with perfect transmission $T=1$ shows low, but finite noise. This is markedly different from the normal

conducting case where, given the shot-noise formula $S_I = (Ve^3/\pi\hbar)T(1-T)$, we would anticipate zero noise in the case of perfect transmission. Furthermore, we see that the larger the transmission the steeper and higher is the noise ascent for small voltages. For high $eV$, the high-transmission curves approach the $T=1$ characteristic. Thus, altogether we see that in this case the description with pure Poissonian shot noise with modified charge quantum is insufficient and the generalization used in the rest of this paper shows special features.

It is instructive to look at the noise curve from a different perspective. Focusing on the $T$ dependence, in Fig. 6, we set voltage as a parameter and plot noise as a function of transmission. The noise develops a maximum at high-transmission values. As noticed before, each curve falls off to a finite residual noise level at $T=1$. For smaller voltages, the maximum becomes more and more pronounced and it seems to be squeezed into the high-transmission regime. For $eV=0.1\Delta$ only channels with very high transmission significantly contribute to the noise.

The explanation of the noise features for high transmission is more involved. From Eq. (4) we see that the noise can be expressed in terms of the variance of $P_n(E,V,T)$, which is the probability for a MAR-process transferring charge quanta $ne$

$$S_I = \frac{4e^2}{h}\int_0^{eV} dE[\langle n^2\rangle - \langle n\rangle^2] = \frac{4e^2}{h}\int_0^{eV} dE\, \mathrm{Var}(n). \quad (5)$$

Thinking of shot noise as partition noise, for a single-mode normal conductor with perfect transmission $T=1$, there is no uncertainty whether a particle is transmitted or reflected. We find zero noise. In the superconducting case, due to perfect transmission, we are still certain about charge transfer taking place but an additional uncertainty is introduced. For high transmission including $T=1$, there are many different MAR processes contributing to charge transport, which is described by the probability distribution $P_n$. This additional uncertainty is the qualitative physical explanation of the finite noise observed in the case of perfect transmission.
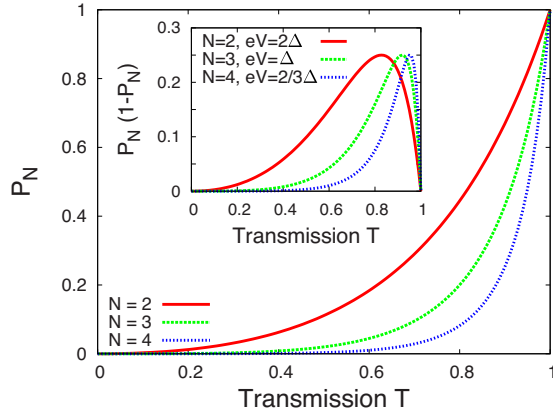
FIG. 7. (Color online) Toy-model probability $P_N$ to transfer $N$ charges at a time as a function of transmission eigenvalue $T$. Inset: expression $P_N(1-P_N)$, that occurs as a term in the second cumulant [Eq. (8)], as a function of transmission eigenvalue $T$.

### *1. Toy model*

To clarify the essential physics, referring to the full computer-algebraic calculation is unsatisfactory. Thus, we will try to explain the basic noise features with the use of the toy model presented before in Ref. 39. Originally, this model was introduced to illustrate how to calculate the cumulant generating function of a weak link with voltage bias in an easy, analytically solvable case. We summarize the basic simplifying assumptions.

We only look at voltages equal to one of the MAR voltages $V_n = 2\Delta/(ne)$ and for each of them we only take into account one MAR process, namely, the most relevant one which transfers

$$N = \left\lfloor \frac{2\Delta}{eV} \right\rfloor + 1 \tag{6}$$

charge quanta. This simplifies the cumulant generating function $\mathcal{C}_{t_0}(\chi)$ to the one of a binomial distribution. Furthermore, in this model, Andreev reflection above the gap is neglected and the Green's function is simplified by assuming a constant density of states above the gap.

The cumulant generating function for the toy model reads

$$\mathcal{C}_{t_0}(\chi) = \frac{2eVt_0}{h}\ln[1 + P_N(e^{iN\chi} - 1)]. \tag{7}$$

For every MAR voltage $V = V_n$, another specific transport process with probability $P_N$ is relevant, Eq. (6). We emphasize that, due to this, the argument of the logarithm in Eq. (7) depends on voltage via the selection of the relevant $P_N$. Figure 7 shows the toy-model probabilities $P_N$ as a function of transmission eigenvalue $T$. For perfect transmission, as we have reduced the system to a binomial distribution involving only a single transport process, each probability is unity. The probabilities for $N \geq 2$ and imperfect transmission are always smaller than in the normal conducting case because a higher-order process is necessary in order to transfer charge. For large charge quanta $N$, very high transmission is necessary, since many Andreev reflections are involved in such a process. Thus, for a larger number of Andreev cycles $N$, i.e.,
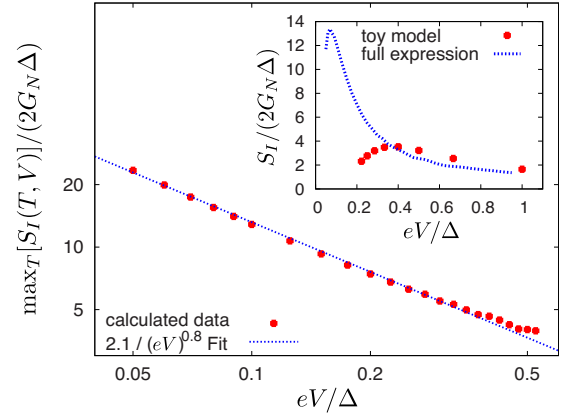


FIG. 8. (Color online) Maximal noise $\max_T[S_I(T,V)]$, optimized with transmission as a parameter, as a function of bias voltage on a double-logarithmic scale for a homogeneous contact between superconductors. The calculated data using the full expression, Eq. (1), are fitted using the given power law. Inset: comparison of the noise results calculated for a $T = 0.97$ homogeneous contact between superconductors as a function of bias voltage using either the full expression or the toy model.

small-voltage bias [Eq. (6)], higher channel transmission is required to obtain non-negligible transfer probability.

The second cumulant

$$c_2 = -\left.\frac{\partial^2}{\partial\chi^2}\mathcal{C}_{t_0}\right|_{\chi=0} = N^2\frac{2eVt_0}{h}P_N(1-P_N) \tag{8}$$

is proportional to the zero-frequency noise $S_I = (2e^2/t_0)[\partial^2\mathcal{C}_{t_0}/\partial\chi^2]_{\chi=0}$, see above. The expression $P_N(1-P_N)$, which matches the one in the traditional shot-noise formula if we replace $T$ by $P_N$, is displayed in the inset of Fig. 7. For large $N$, i.e., small voltage, the maximum is shifted and squeezed into the high-transmission regime.

So, altogether, we distinguish two mathematical ingredients to the noise. One is the expression $P_N(1-P_N)$ that we just discussed. Additionally, there is the prefactor $N^2(2eVt_0/h)$. In the small-voltage regime, where $N \simeq 2\Delta/eV$ [Eq. (6)], it results in noise enhancement that behaves approximately like $1/V$. As the noise is determined by the product of both parts, for a fixed-transmission coefficient, there will be a voltage regime where the noise gets enhanced by lowering the applied voltage bias. However, at some voltage, or conversely for some $N$, $P_N(1-P_N)$ will overcompensate this increase and reduce the noise again. To summarize, the toy model still explains noise enhancement by an increased charge quantum. The decrease in noise at very low voltage follows from the overcompensation of this effect by the decrease in transfer probability in the expression $P_N(1-P_N)$.

In the inset of Fig. 8, for comparison, the noise calculated using the full expression and the toy model at MAR voltages, is presented in a single plot. The simplified model qualitatively shows the basic features of our numerical calculation. Nevertheless, there is a huge quantitative difference. Thus, we realize that the toy model is qualitatively sufficient but it
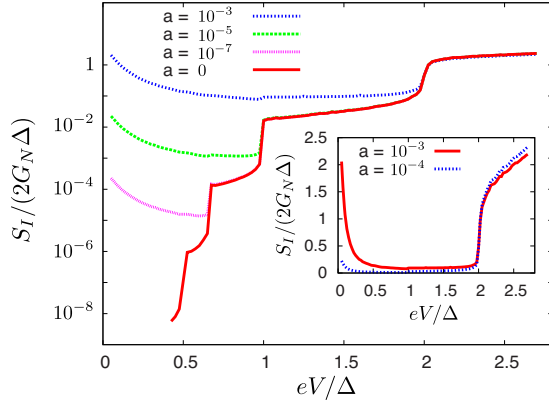
FIG. 9. (Color online) Noise $S_I$ on a logarithmic scale as a function of bias voltage, at zero temperature, for a rough superconducting tunnel junction characterized by the transmission eigenvalue distribution $\rho(T) = a\delta(T - T_1) + (1 - a)\delta(T - T_2)$, $T_1 = 0.986$ and $T_2 = 0.01$. The different curves refer to different pinhole fractions $a$ within all transport channels. Inset: linear noise scale.

fails dramatically to provide quantitative results. Thus, for quantitative calculations, the extensive calculation, used in this paper, is essential.

### 2. What is driving the noise increase?

We can ask the question: what is the maximal noise at a given voltage? This means, for fixed voltage bias, we use the transmission eigenvalue as a parameter to find the maximal value. In the toy model, Fig. 7, $\max_T[P_N(1 - P_N)]$ is always $1/4$. Thus, here, the maximal noise $\max_T[S_I(T, V)]$ depends only on the prefactor in Eq. (8). Consequently, for small voltages, it approximately scales like $1/V$, see the discussion above.

For the full theory, in Fig. 8 the maximal noise $\max_T[S_I(T, V)]$ is plotted against voltage bias on a double-logarithmic scale. In the small-voltage regime, the data can be fitted well using a power law. We find

$$\max_T[S_I(T, V)] \propto \frac{1}{V^{0.8}}.$$

Thus, although quantitative statements resulting from the toy model and from the full expression differ significantly, we see that the maximal noise at given voltage follows a similar power law with an exponent of 0.8 instead of unity. Hence, even in the much more complicated situation, including multiple MAR processes, the inherent $1/V$ dependence, which basically results from the increased charge quanta, seems to play a major role.

### B. Noise of rough superconducting tunnel junctions

We now return to the model of Sec. III C. There, we looked at a rough superconducting tunnel junction with eigenvalue distribution given by Eq. (3). Here, we are concerned with the noise generated in this kind of junction. Figure 9 shows the result.

In contrast to a normal tunnel junction, we see a dramatic change in the noise characteristic due to very few pinholes

with an enormous noise increase at small voltages. As in the case of leakage current, at a certain point in the subgap regime, the pinholes begin to dominate the noise characteristic but here the total noise can become huge. Together with our results in Sec. III, this demonstrates one of our central results: although a junction possessing few pinholes might still have only a small total leakage current, it can lead to enormous current fluctuations in the low-voltage regime. As pointed out before, sensitive measurements of the leakage current will provide an estimate on the amount of pinholes that might be contained in the considered junction.

The considered pinhole-transmission eigenvalue of $T = 0.986$ is chosen in order to display all structure at voltages down to $eV = 0.05\Delta$. Nevertheless, analogous to Sec. IV A, we can add two more aspects: first, for smaller voltages than resolved in Fig. 9, the noise will show a maximum and then will fall off again. Second, considering higher values of transmission will lead to an even steeper and higher ascent, starting at smaller voltages.

## V. FULL COUNTING STATISTICS OF PINHOLES

We will investigate the FCS of charge transport through pinholes of a rough superconducting tunnel junction. Given the CGF in Eq. (1), the FCS is calculated by Fourier transformation, see Sec. II. Using this insight into the transport process, we will discuss a possible model of high-transmission channels as microscopic origin of two-level current fluctuators.

### A. Resolution of structure in the full counting statistics

To determine the probability distribution $P_{t_0}(N)$, we have to set the measurement time $t_0$. In general, the calculation of the CGF for a voltage-biased Josephson junction is significantly complicated due to the ac Josephson effect.[38,39] In order to make computation feasible and to avoid interpretation difficulties of arising "negative probabilities" in the superconducting system,[42] $t_0$ must be sufficiently longer than the inverse of the Josephson frequency $T_J = h/2eV$. (See Ref. 39 for further details). Consequently $T_J$ sets a time scale in our approach and there is a lower bound for the measurement time $t_0$.

We consider a contact with transmission eigenvalue $T = 0.936$ at low-bias voltage $eV = 0.3\Delta$, where qubits might be operated, and take into account two different measurement times $t_0 = 10 T_J$ and $t_0 = 100 T_J$. Figure 10 shows the results: for the long measurement time the FCS is Gaussian. In contrast, for $t_0 = 10 T_J$ we see a rich comb structure.

We will discuss this comb structure and its origin in detail later on. Here, we want to point out that this structure turns into a Gaussian for long measurement time $t_0$. This is as we would expect: if we sum the number of transferred charges over a very long time it will become possible, instead of considering individual MAR processes with their specific probabilities, to just assign an average likelihood for one elementary charge quantum to be transferred. Thus, in the long measurement time limit, transport can be described by a sum of many independent and identically distributed events
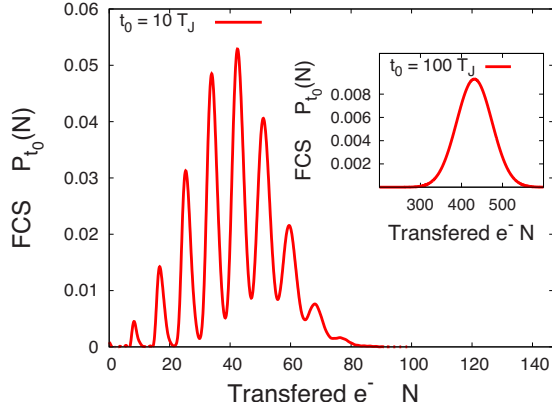
FIG. 10. (Color online) FCS for a transport channel between superconductors with transmission $T=0.936$ and voltage bias $eV=0.3\Delta$ at measurement time $t_0=10T_J$. Inset: measurement time $t_0=100T_J$.

what results in a Gaussian. This is the essence of the central limit theorem used in statistical physics. Indeed, the problem above can be related to the *quasiergodic hypothesis*. Hence, it is clear that for very long measurement times the comb structure, due to individual, discrete transport processes, is washed out.

For significantly higher voltages, such as $eV=1.5\Delta$, the most relevant transport processes transfer much smaller charge quanta. It turns out that consequently, in this case, discrete structures in the FCS cannot be resolved using the time interval $t_0=10T_J$. Despite these limitations concerning $t_0$, we can resolve structure in the FCS for a limited parameter window.

### B. Pinholes as junction resonators?

#### 1. Motivation

We are now coming back to the questions whether pinholes might explain decoherence from junction resonators in-phase qubits or $1/f$ noise.[12–14] Thinking of the different possible MAR processes, which transfer different sizes of charge quanta, a pinhole might introduce current fluctuators: imagine a high-transmission channel, i.e., a pinhole hidden in the junction. Two different MAR processes $A$ and $B$ transfer charge in two different quanta $n_Ae$ and $n_Be$. Thus, we might think of two current states $|A\rangle$ and $|B\rangle$; each of them carry charge using only one of the distinct MAR processes $A$ and $B$, respectively. Due to the differently sized Andreev clusters being transferred, the two states will cause two different currents. In principle, the mechanism is similar to the idea of charge trapping,[14] where a trapped charge blocks tunneling through a transport channel. There, one introduces an untrapped state $|\tau_u\rangle$ causing high current and a trapped state $|\tau_t\rangle$ causing low current. In comparison, we consider two current states $|A\rangle$ and $|B\rangle$ corresponding to charge transport by two different MAR processes and thereby causing two distinct currents.

#### 2. Calculation

We investigate whether this scenario results from a pinhole model. If this was the case, we would expect to find two



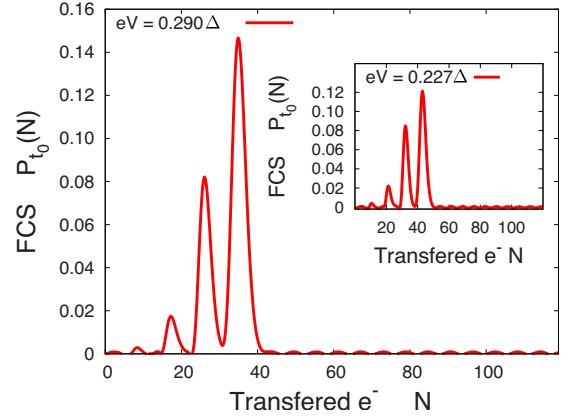FIG. 11. (Color online) FCS for a transport channel between superconductors with transmission eigenvalue $T=0.99$ and voltage bias $eV=0.290\Delta$. Inset: $eV=0.227\Delta$. The measurement time is $t_0=4T_J$.

distinct peaks in the FCS, where the first one refers to charge transport due to MAR process $A$ and the second one corresponds to MAR process $B$, each within the time interval $t_0$. Hence, let us see whether we find parameters that result in such an FCS.

We consider very high-transmission channels, for instance, $T=0.99$ and calculate the FCS for this transmission eigenvalue at two subgap voltages. The results are shown in Fig. 11. We find two very pronounced peaks in the FCS. Note that here the measurement time is very short but, despite some artifacts in the diagrams, the distribution still has a normalization close to unity.

#### 3. Attempted interpretation in terms of two-level fluctuator

Given these pronounced peaks, does this result indicate a scenario where a pinhole via its different MAR processes might actually introduce a two-level current fluctuator? If we assume so, we associate the first peak with the case where charge transport is carried by MAR process $A$, i.e., charge transport in quanta of $n_Ae$ only. Accordingly the second peak refers to the case where transport takes places via MAR process $B$, using charge quanta $n_Be$.

Taking a closer look at Fig. 11 reveals a sharp boundary for the appearance of peaks toward large total charge numbers $N$. In contrast, to the left, i.e., toward smaller $N$, we see small peaks next to the dominating ones. In fact, for a given voltage, there is a *lower* threshold for the MAR order, i.e., a *lower* bound on the minimal charge cluster being transferred in a single MAR process. Furthermore, in addition to the dominant processes $A$ and $B$, there will also be finite probability for MAR of higher order, i.e., current flow via even larger quanta than $n_Ae$ or $n_Be$. So according to the two-level interpretation, identifying each peak with charge transport due to different MAR processes, we would expect this boundary to be reversed, namely: a sharp boundary for the existence of peaks toward small $N$ due to the lower bound on the charge cluster size, and additionally, little peaks toward large $N$ due to the finite probability for MAR of higher order than the two dominant ones, $A$ and $B$.

The second aspect is the spacing between the peaks. For the distributions in Fig. 11, the distance is slightly larger than the smallest possible charge quantum ($\lfloor 2\Delta/eV \rfloor + 1$), i.e., for the main panel it is 7 and 9 for the inset. With respect to the MAR threshold, this is roughly the size of the average charge quantum that we would expect to be transferred by a single Andreev cluster. In Fig. 11, from the number of transferred charges and the minimal Andreev cluster size, we infer that, within the measurement time $t_0$, roughly five MAR processes contributed to the rightmost peaks. In the above two-level scenario, $A$ and $B$ are adjacent MAR processes meaning their transferred charge quanta differ only in one elementary charge. Thus, if a pinhole introduced a two-level current fluctuator where each peak refers to current flow via distinct MAR processes $A$ and $B$, in Fig. 11 we would expect a peak spacing of $\Delta N = 5$ rather than a value larger than ($\lfloor 2\Delta/eV \rfloor + 1$). This makes the two-level fluctuator hypothesis inconsistent.

#### 4. Alternative, consistent interpretation

Thus, the structure we have seen in the FCS of a pinhole does not correspond to the scenario of a two-level current fluctuator as suggested above. In fact, the description of the probability distribution becomes consistent if we identify each peak with the number of attempts being successful to transmit an Andreev cluster: within the measurement time $t_0$ we might think of a total number of attempts to transfer charge cluster, where the actual size of the quantum might differ due to the individual, possible MAR processes. In the distributions of Fig. 11, each rightmost peak corresponds to the case where every attempt is successful to transfer an Andreev cluster so we get the sharp boundary observed for the appearance of peaks toward large $N$. The next peak to the left corresponds to the case where exactly one attempt fails and so on. Thus, the peaks are naturally separated by a distance larger than ($\lfloor 2\Delta/eV \rfloor + 1$), namely, the average Andreev cluster size transferred in case of a successful attempt. As the actual size of successfully transmitted clusters might differ due to the individual MAR processes, the pronounced peaks are broadened. The comb structure in Fig. 10 can be explained the same way. Here, in contrast to Fig. 11, due to smaller transmission, the case where every attempt is successful is not the most likely one.

#### 5. Conclusion

To summarize this section, we have discussed the possibility of a pinhole to introduce a two-state current fluctuator due to its different MAR transport processes. This is conceptually similar to the mechanism of charge trapping, Ref. 14. Although at first sight it is suggestive to relate the observed peak structure to distinct MAR processes, a more detailed analysis suggests a very different but consistent interpretation in terms of successful transport attempts of Andreev cluster. Taking this into account, we see no clear evidence that a pinhole might be a microscopic origin for introducing two-level current fluctuators. Charge trapping in junctions is probably one of the most relevant mechanisms. However, it might be, in particular, interesting to think about such a process opening and closing a very high-transmission channel, i.e., a pinhole. Due to the large charge quanta being transferred, the process of trapping and untrapping might result in high magnitudes of current fluctuations. This picture may change if electron-electron interaction is included, given that the large charge quanta in a pinhole may efficiently block large parts of the junction.

A very intuitive picture might be an occupied upper Andreev bound state,[43] that causes a repulsion within the channel. Nevertheless, in the case of voltage bias, such a state with energy $E_J = \Delta \{ 1 - T \sin^2[\phi(t)/2] \}^{1/2}$, where $\phi(t)$ is the superconducting phase, might be adiabatically carried above the gap within only one cycle of $E_J$ directly after population. Further research might clarify this scenario.

### VI. CONCLUSION

We have investigated voltage-biased *rough superconducting tunnel junctions* containing some high-transmission channels, pinholes. We have accomplished this using the method of full counting statistics formulated within the non-equilibrium Keldysh Green's functions technique. Based on this microscopic approach, we were able to properly quantify physical effects due to low- *and high*-transmission channels in a single junction.

By exploring *leakage current* of such systems, we observed that a tunnel junction may contain much fewer pinholes than previously speculated.[25] We further demonstrated how highly sensitive current measurements can clarify the existence of pinholes. We pointed out that existing current measurements done for junctions of the superconducting qubit devices[31] do not strictly rule out the existence of a hidden pinhole.

Furthermore, we examined *noise* properties. We demonstrated that even very few pinholes give rise to a drastic increase in the noise in the very low subgap voltage regime. Thus, although a junction possessing few pinholes might still have just a small total leakage current, it can lead to enormous current fluctuations in the low-voltage regime. Although details of this noise enhancement, comprising contributions of several MAR processes, turned out to be quite complicated, we proposed that the physical essence of the observed noise boost still lies in the increased charge quantum that is transferred. To do this, we compared the explicit noise calculation to a simplified model. This showed qualitative agreements and thus illuminated some essential features but failed quantitatively, therefore demonstrating the need of a full calculation.

Finally, we investigated the FCS of charge transport through pinholes. Despite limitations concerning the measurement time $t_0$, we could resolve non-Gaussian structure in the FCS for a limited parameter window. We discussed a possible model of high-transmission channels as a microscopic origin of two-level current fluctuators. Indeed, for certain voltage parameters, the FCS shows a two-level peak structure. From a more detailed analysis we inferred that this structure *cannot* be related to charge transport by distinct MAR processes. Thus, given the dc part of the probability distribution, we find no evidence that a pinhole might intro-

duce an additional source of two-level current fluctuators. We presented an alternative, consistent interpretation of the observed peak structure in terms of successful transmission attempts of Andreev clusters.

So far, our approach is limited to the stationary or quasistationary case. Improvements on this might incorporate time dependence into the Keldysh Green's function approach. This may permit a more rigorous discussion of finite-frequency noise with respect to pinholes. Recently, first steps toward the discussion of time dependence using this method have been made.[44] Also, electron-electron interactions describing the traditional $1/f$ noise scenario for Josephson junctions should be included.

## APPENDIX: DETAILS OF THE CALCULATION

From its definition in Sec. II, the FCS of electric transport is determined by the statistics of $\int_0^{t_0} dt I(t)$, where $I(t)$ is the current operator. In general, for a system determined by a Hamiltonian $H_{sys}$, the back action due to the measurement process must be carefully taken into account.[35] As proposed in Ref. 33, the result for the CGF $\mathcal{C}(\chi)$, see Sec. II, can be formulated using Keldysh time ordering $T_{\tilde{c}_k}$ as

$$e^{\mathcal{C}(\chi)} = \left\langle T_{\tilde{c}_K} e^{-\chi/2e \int_{\tilde{c}_k} d\tau I(\tau)} \right\rangle, \tag{A1}$$

where $I(\tau) = \pm I$ for $\tau$ on the upper (lower) branch of the Keldysh contour $\tilde{c}_k$, see, for example, Ref. 37. $\chi$ is usually called counting field.

On the other hand, using the usual field operators $\psi^\dagger$ and $\psi$, the single-particle Hamiltonian $h_{sys}$ with $H_{sys} = \int d^3 x \psi^\dagger(\mathbf{x}) h_{sys}(\mathbf{x}) \psi(\mathbf{x})$ and a time-dependent perturbation $\frac{\chi}{2e} I(\tau) = \pm \frac{\chi}{2e} \int d^3 x \psi^\dagger(\mathbf{x}, t) j(\mathbf{x}) \psi(\mathbf{x}, t)$, we can formulate the equation of motion[37] for the counting field-dependent Green's function in Keldysh space $\check{G}(1, 1'; \chi)$,

$$\left[ i \frac{\partial}{\partial t} - h_{sys}(\mathbf{x}) + \frac{\chi}{2e} \check{\tau}_k j(\mathbf{x}) \right] \check{G}(1, 1'; \chi) = \delta(1 - 1'). \tag{A2}$$

$j(\mathbf{x}) = [\nabla F(\mathbf{x})] \lim_{\mathbf{x} \to \mathbf{x}'} \frac{ie}{2m} (\nabla_{\mathbf{x}} - \nabla_{\mathbf{x}'})$ denotes the current-density operator yielding the current through a certain cross section determined by $F(\mathbf{x})$. For instance, $F(\mathbf{x})$ might be zero to the left and one to the right of this surface, and change on a length scale in between such that $\nabla F(\mathbf{x})$ is nonzero only along the cross section and always perpendicular to it. The matrix $\check{\tau}_k$ takes into account the reversed sign of $\hat{I}(\tau)$ on the two branches of $\tilde{c}_k$. Given a solution of Eq. (A2), the current, now depending on the counting field, reads

$$I(\chi, t) = \int d^3 x \, \mathrm{Tr}[\check{\tau}_k j(\mathbf{x}) \check{G}(1, 1'; \chi)]|_{1 \to 1'}. \tag{A3}$$

By diagrammatic expansion of $\check{G}(1, 1'; \chi)$, Eq. (A1) can be related to Eq. (A3): $\frac{\partial}{\partial \chi} \mathcal{C}(\chi) = \frac{i}{e} \int_0^{t_0} dt I(\chi, t)$. Thus, the CGF is connected to a transport problem in terms of Keldysh Green's functions.

Our problem here is to describe transport through rough superconducting tunnel junctions. Finding exact solutions for Green's functions like Eq. (A2), is almost impossible. For the two superconductors involved here, quasiclassical and dirty-limit approximation are adequate approximations, see, for instance, Ref. 37. The circuit theory of mesoscopic transport[45,46] is an applicable formulation of the theory of nonequilibrium superconductivity for systems where these two approximations can be applied. The idea of this theory is to subdivide a device into terminals, nodes, and connectors, and describe transport in terms of a *matrix current* that reflects the $4 \times 4$ Keldysh-Nambu matrix structure due to superconductivity [see, for instance, Ref. 37 and note $\check{G}(1, 1'; \chi)$ in Eq. (A3)]. The key element in this theory is the *arbitrary connector* introduced in Ref. 47 which is represented by a set of transmission eigenvalues $\{T_m\}$. Given the Green's functions $\check{G}_{1(2)}(t, t')$, on the right and the left of this contact, the matrix current reads

$$\check{I}(t, t') = -\frac{e^2}{\pi} \sum_m \frac{2 T_m [\check{G}_1 \otimes G_2]}{4 + T_m (\{G_1 \otimes G_2\} - 2)}, \tag{A4}$$

where $\otimes$ denotes a convolution over the intermediate time $(A \otimes B)(t, t') = \int dt'' A(t, t'') B(t'', t')$ and $[\cdot, \cdot]$ ($\{\cdot, \cdot\}$) is the (anti)commutator. Analogous to Eq. (A3), the current is $I(t) = \frac{1}{4e} \mathrm{Tr}[\tau^3 \check{I}(t, t)]$.

For a rough superconducting tunnel junction, the oxide layer, possessing a set of transmission channels with transmission $\{T_m\}$, has a width much smaller than the coherence length $\xi_0$. According to circuit theory,[47] such a short junction can be modeled by two voltage-biased superconducting terminals separated by one single connector with matrix current, Eq. (A4). It is essential to note that Eq. (A4) is derived using quasiclassical Zaitsev boundary conditions which properly describe boundaries between metals, see Ref. 48.

The two terminals are described by two Green's functions $\check{G}_{1(2)}$ in Keldysh($\hat{}$)-Nambu($\bar{}$) space.[37] We set the chemical potential of $\check{G}_2$ to zero, i.e., $\check{G}_2 = \check{G}_S(t - t')$ where $\check{G}_S(t - t')$ is the bulk solution for the superconductor at zero potential, see Ref. 37. The constant voltage bias $V$, causing a time-dependent superconducting phase, is completely incorporated into $\check{G}_1$ by a rotation in Nambu space $\check{G}_1(t, t') = e^{i \phi(t) \bar{\sigma}^3/2} \check{G}_S(t - t') e^{-i \phi(t') \bar{\sigma}^3/2}$ where $\phi(t) = \phi_0 + (2eV/\hbar) t$ and $\bar{\sigma}^3$ is the Pauli matrix. The counting field $\chi$ in Eq. (A2) is considered as a boundary condition $\check{G}_1(\chi; t, t') = e^{-i \chi \check{\tau}_k/2} \check{G}_1(t, t') e^{i \chi \check{\tau}_k/2}$, see Ref. 42. Using $\check{G}_{1(2)}$, Eq. (A4) and $\frac{\partial}{\partial \chi} \mathcal{C}(\chi) = \frac{i}{e} \int_0^{t_0} dt I(\chi, t)$, we can calculate the CGF.

The detailed calculation of this problem for a single-mode contact was done in Refs. [38] and [39]. The computation for the multimode case, relevant here, is analogous despite the sum over different transmission coefficients $\{T_m\}$ in Eq. (A4). The result for the CGF in this case is given in Eq. (1), where the lengthy formulas for the probabilities $P_n(E, V, T)$ are identical to those in Ref. [39] and can be found there.

---

*fwilhelm@iqc.ca

[1] J. Clarke and F. K. Wilhelm, Nature (London) **453**, 1031 (2008).

[2] Y. Makhlin, G. Schön, and A. Shnirman, Rev. Mod. Phys. **73**, 357 (2001).

[3] J. R. Friedman, V. Patel, W. Chen, S. K. Tolpygo, and J. E. Lukens, Nature (London) **406**, 43 (2000).

[4] C. H. van der Wal, A. C. J. ter Haar, F. K. Wilhelm, R. N. Schouten, C. J. P. M. Harmans, T. P. Orlando, S. Lloyd, and J. E. Mooij, Science **290**, 773 (2000).

[5] I. Chiorescu, Y. Nakamura, C. J. P. M. Harmans, and J. E. Mooij, Science **299**, 1869 (2003).

[6] Y. Nakamura, Y. A. Pashkin, and J. S. Tsai, Nature (London) **398**, 786 (1999).

[7] Y. A. Pashkin, T. Yamamoto, O. Astafiev, and Y. Nakamura, Nature (London) **421**, 823 (2003).

[8] J. M. Martinis, S. Nam, J. Aumentado, and C. Urbina, Phys. Rev. Lett. **89**, 117901 (2002).

[9] Y. Yu, S. Han, X. Chu, S.-I. Chu, and Z. Wang, Science **296**, 889 (2002).

[10] R. McDermott, R. W. Simmonds, M. Steffen, K. B. Cooper, K. Cicak, K. D. Osborn, S. Oh, D. P. Pappas, and J. M. Martinis, Science **307**, 1299 (2005).

[11] F. C. Wellstood, C. Urbina, and J. Clarke, Appl. Phys. Lett. **50**, 772 (1987).

[12] P. Dutta and P. M. Horn, Rev. Mod. Phys. **53**, 497 (1981).

[13] M. B. Weissman, Rev. Mod. Phys. **60**, 537 (1988).

[14] D. J. Van Harlingen, T. L. Robertson, B. L. T. Plourde, P. A. Reichardt, T. A. Crane, and J. Clarke, Phys. Rev. B **70**, 064517 (2004).

[15] M. Muck, M. Korn, C. Mugford, J. Kycia, and J. Clarke, Appl. Phys. Lett. **86**, 012510 (2005).

[16] F. Deppe, M. Mariantoni, E. P. Menzel, S. Saito, K. Kakuyanagi, H. Tanaka, T. Meno, K. Semba, H. Takayanagi, and R. Gross, Phys. Rev. B **76**, 214503 (2007).

[17] R. H. Koch, D. P. DiVincenzo, and J. Clarke, Phys. Rev. Lett. **98**, 267003 (2007).

[18] L. Faoro and L. B. Ioffe, Phys. Rev. Lett. **100**, 227005 (2008).

[19] M. Constantin and C. C. Yu, Phys. Rev. Lett. **99**, 207001 (2007).

[20] S. Datta, *Electronic Transport in Mesoscopic Systems* (Cambridge University Press, Cambridge, 2005).

[21] J. Eroms, L. C. van Schaarenburg, E. F. C. Driessen, J. H. Plantenberg, C. M. Huizinga, R. N. Schouten, A. H. Verbruggen, C. J. P. M. Harmans, and J. E. Mooij, Appl. Phys. Lett. **89**, 122516 (2006).

[22] S. Oh, K. Cicak, R. McDermott, K. B. Cooper, K. D. Osborn, R. W. Simmonds, M. Steffen, J. M. Martinis, and D. P. Pappas, Supercond. Sci. Technol. **18**, 1396 (2005).

[23] P. Dieleman, H. G. Bukkems, T. M. Klapwijk, M. Schicke, and K. H. Gundlach, Phys. Rev. Lett. **79**, 3486 (1997).

[24] G. Zaránd, G. T. Zimányi, and F. Wilhelm, Phys. Rev. B **62**, 8137 (2000).

[25] A. W. Kleinsasser, R. E. Miller, W. H. Mallison, and G. B. Arnold, Phys. Rev. Lett. **72**, 1738 (1994).

[26] A. F. Andreev, Sov. Phys. JETP **19**, 1228 (1964).

[27] G. E. Blonder, M. Tinkham, and T. M. Klapwijk, Phys. Rev. B **25**, 4515 (1982).

[28] T. M. Klapwijk, G. E. Blonder, and M. Tinkham, Physica B **109-110**, 1657 (1982).

[29] M. Octavio, M. Tinkham, G. E. Blonder, and T. M. Klapwijk, Phys. Rev. B **27**, 6739 (1983).

[30] Y. Blanter and M. Büttiker, Phys. Rep. **336**, 1 (2000).

[31] R. W. Simmonds, K. M. Lang, D. A. Hite, S. Nam, D. P. Pappas, and J. M. Martinis, Phys. Rev. Lett. **93**, 077003 (2004).

[32] M. Neeley, M. Ansmann, R. C. Bialczak, M. Hofheinz, N. Katz, E. Lucero, A. O'Connell, H. Wang, A. N. Cleland, and J. M. Martinis, Nat. Phys. **4**, 523 (2008).

[33] Y. V. Nazarov, Ann. Phys. (Leipzig) **8**, 507 (1999).

[34] L. S. Levitov, H. Lee, and G. B. Lesovik, J. Math. Phys. **37**, 4845 (1996).

[35] Y. V. Nazarov and M. Kindermann, Eur. Phys. J. B **35**, 413 (2003).

[36] S. Pilgram, A. N. Jordan, E. V. Sukhorukov, and M. Büttiker, Phys. Rev. Lett. **90**, 206801 (2003).

[37] J. Rammer and H. Smith, Rev. Mod. Phys. **58**, 323 (1986).

[38] J. C. Cuevas and W. Belzig, Phys. Rev. Lett. **91**, 187001 (2003).

[39] J. C. Cuevas and W. Belzig, Phys. Rev. B **70**, 214512 (2004).

[40] K. M. Lang, S. Nam, C. U. J. Aumentado, and J. M. Martinis, IEEE Trans. Appl. Supercond. **13**, 989 (2003).

[41] M. Steffen, M. Ansmann, R. McDermott, N. Katz, R. C. Bialczak, E. Lucero, M. Neeley, E. M. Weig, A. N. Cleland, and J. M. Martinis, Phys. Rev. Lett. **97**, 050502 (2006).

[42] W. Belzig and Y. V. Nazarov, Phys. Rev. Lett. **87**, 197006 (2001).

[43] J. M. Martinis, arXiv:cond-mat/0402415 (unpublished).

[44] M. Vanević, Y. V. Nazarov, and W. Belzig, Phys. Rev. Lett. **99**, 076601 (2007).

[45] Y. V. Nazarov, Phys. Rev. Lett. **73**, 134 (1994).

[46] Y. V. Nazarov, Phys. Rev. Lett. **73**, 1420 (1994).

[47] Y. V. Nazarov, Superlattices Microstruct. **25**, 1221 (1999).

[48] A. V. Zaitsev, Sov. Phys. JETP **59**, 1015 (1984).